

This is a copy of the published version, or version of record, available on the publisher's website. This version does not track changes, errata, or withdrawals on the publisher's site.

Cryogenic testing of the integrated Ariel space telescope: design of the optical test equipment

Robert Spry, Manuel Abreu, Keith Nowicki, Neil Bowles, Maisie Rashman, Cédric Pereira, Jake Hutchinson, David Miguel Ventura de Castro Alves, Rory Evans, Robert Watkins, Waqas Mir, John-Paul Walker, Ioannis Argyriou, Joss Guy, Juergen Schmoll, Chris Davison, Henry Eshbaugh, Alexandre Cabral, Rachel Drummond, Lucile Desjonquieres, Mark Anderson, Georgia Bishop, Paul Eccleston, Enzo Pascale, Andrew Caldwell, Giovanna Tinetti

Published version information:

Citation: Robert Spry et al., Cryogenic testing of the integrated Ariel space telescope: design of the optical test equipment, Proceedings Volume 13092, Space Telescopes and Instrumentation 2024: Optical, Infrared, and Millimeter Wave; 130924V (2024)

DOI: <https://doi.org/10.1117/12.3020185>

Copyright 2024 Society of Photo-Optical Instrumentation Engineers (SPIE). One print or electronic copy may be made for personal use only. Systematic reproduction and distribution, duplication of any material in this publication for a fee or for commercial purposes, and modification of the contents of the publication are prohibited.

This version is made available in accordance with publisher policies. Please cite only the published version using the reference above. This is the citation assigned by the publisher at the time of issuing the APV. Please check the publisher's website for any updates.

This item was retrieved from **ePubs**, the Open Access archive of the Science and Technology Facilities Council, UK. Please contact epublications@stfc.ac.uk or go to <http://epubs.stfc.ac.uk/> for further information and policies.

Cryogenic testing of the integrated Ariel space telescope: Design of the optical test equipment

Robert Spry^{*a}, Manuel Abreu^b, Keith Nowicki^a, Neil Bowles^a, Maisie Rashman^a, Cédric Pereira^b, Jake Hutchinson^a, David Miguel Ventura de Castro Alves^b, Rory Evans^a, Robert Watkins^a, Waqas Mir^a, John-Paul Walker^a, Ioannis Argyriou^c, Joss Guy^d, Juergen Schmoll^d, Chris Davison^d, Henry Eshbaugh^a, Alexandre Cabral^b, Rachel Drummond^e, Lucile Desjonqueres^e, Mark Anderson^e, Georgia Bishop^e, Paul Eccleston^e, Enzo Pascale^f, Andrew Caldwell^e, Giovanna Tinetti^g

^aDepartment of Physics, University of Oxford, UK; ^bInstitute of Astrophysics and Space Sciences, University of Lisbon; ^cInstitute of Astronomy, KU Leuven, Belgium; ^eSTFC RAL Space Rutherford Appleton Laboratory; ^fDipartimento di Fisica, La Sapienza Università di Roma, Italy; ^gDepartment of Physics and Astronomy, UCL, UK

* robert.spry@physics.ox.ac.uk; phone +44 1865272895

ABSTRACT

In this proceeding, we present the development of the Optical Ground Support Equipment (OGSE) used for payload-level testing of the Ariel space mission. Ariel is an ESA mission that will use the transit spectroscopy method to observe the atmospheres of nominally ~ 1000 exoplanets. Ariel is a 1 m class cryogenic (~ 40 K) space telescope that will be placed in a halo orbit around the Earth-Sun L2 point. To detect atmospheric molecular absorption features, Ariel will produce medium-resolution spectra ($R \geq 15$) using three spectroscopic channels covering $1.1 - 7.9 \mu\text{m}$ as well as having photometric channels covering $0.5 - 1.1 \mu\text{m}$.

To achieve Ariel's science goals, the payload requires detailed calibration and performance verification. The payload-level performance verification of the Ariel payload will take place in 2026 in a 5-meter vacuum chamber at the Rutherford Appleton Laboratory's Space Instruments Test Facility. The payload will be enclosed in a Cryogenic Test Rig (CTR) to provide a space-like (~ 35 K) thermal environment and is illuminated by the OGSE. The OGSE provides point as well as extended source illumination across Ariel's full wavelength range. The OGSE design also includes a series of mechanisms and features to enable the various illumination conditions required to test Ariel.

Here we report design updates to the OGSE after a preliminary design review (PDR). Since PDR, there have been substantial revisions to the OGSE architecture. In this proceeding, we describe the evolution of the OGSE architecture. The updated OGSE design will then be presented.

Keywords: Ariel, Ground calibration, Infrared, Space Telescope, Optical Ground Support Equipment (OGSE), Exoplanets

1 INTRODUCTION

1.1 The Ariel mission

Ariel will use the transit/eclipse spectroscopy method to observe the atmospheres of ~ 1000 exoplanets. This will enable demographic studies of exoplanet atmospheres for the first time. Further details on the mission's science case can be found in [1]. The Ariel payload features a $\sim 1\text{m}$ off-axis Cassegrain telescope. The telescope then feeds light to two instruments: Ariel InfraRed Spectrometer (AIRS) and the Fine Guidance Sensor (FGS) covering $7.5 - 1.95$ and 1.95 to 0.5 microns respectively. AIRS contains two spectroscopic channels and FGS contains three photometric channels as well as one spectroscopic channel. Using a series of dichroics, simultaneous illumination of all instrument channels is achieved.

1.2 Payload test flow

To enable Ariel's science goals of characterising ~1000 exoplanet atmospheres, Ariel's performance must be verified on ground. Moreover, calibration products must be developed which enable the interpretation and detrending of Ariel's science data. The performance verification and calibration of Ariel will be performed at component, unit, system and, finally, payload level. Tests are conducted at the lowest possible level and results are verified at higher levels where possible. This document covers the payload-level testing of Ariel using the Optical Ground Support Equipment (OGSE).

In this proceeding, we give an overview of the design of the equipment used to test the integrated Ariel payload. The OGSE has a series of sources and mechanisms, with each combination providing different illumination conditions at the focal plane. However, at payload level the range of illumination conditions is restricted by design. For example, the instruments' prisms prevent flat illumination of the focal planes. Moreover, because of this, it is critical that measurements are made at the lowest possible level. Certain tests are, however, only measurable at payload level such as ghosts and instrument co-alignment. Further details on the planned tests and methods used to test them are described in [2].

1.3 Payload testing configuration

To perform these tests, the payload will be tested in the configuration shown in Figure 1 and Figure 2. Payload-level testing will occur in the 5m STC 2 chamber at RAL Space. A test beam is generated by the OGSE illumination module which sits outside the main 5m chamber. To compensate for the offset between the illumination module output and the payload line of sight, a periscope (Z-fold) is used. The test beam then passes into the telescope and common optics where the light is split by a series of dichroics to the different instruments (AIRS and FGS). Further details on the payload and instrument architecture can be found in [1, 3, 4].

In this proceeding, we will describe the equipment used for the payload-level testing.

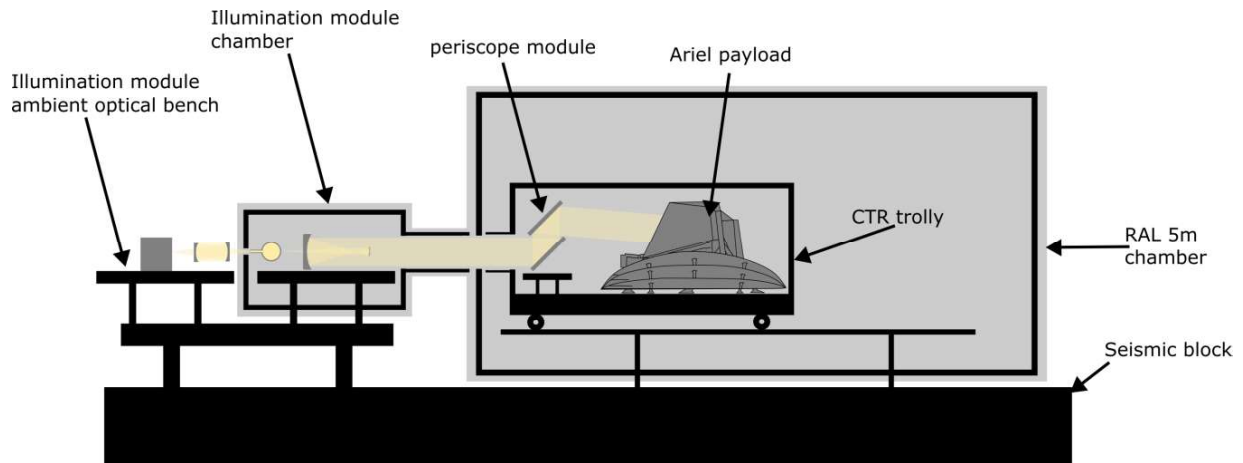


Figure 1: OGSE end-to-end architecture illustrating the 5 m vacuum chamber on the right containing the Ariel payload, CTR trolley and the periscope OGSE subassembly. The OGSE illumination module is shown on the left.

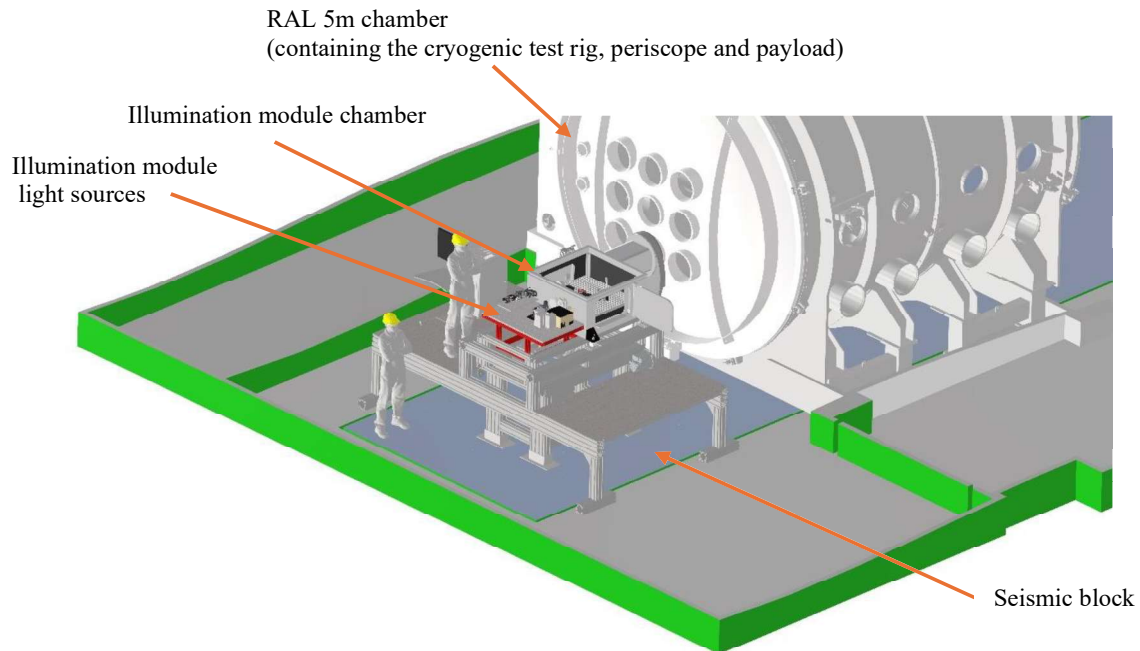


Figure 2: The OGSE illumination module integrated at the RAL Space facility

The Ariel OGSE consists of two modules:

- The illumination module – contains the light sources, reference detectors, an integrating sphere and expansion optics. This generates a $\frac{1}{4}$ aperture collimated beam ($\sim 30\text{cm}$ diameter).
- The periscope – a highly adjustable system capable of redirecting the illumination module output to the payload line of sight.

In addition to the OGSE modules, critical to the payload level testing is the cryogenic test rig (CTR) provided by RAL Space. The CTR consists of an ambient trolley and a cryogenic 35 K shroud. This provides a flight-like radiative environment to enable thermal balance testing and calibration in a representative thermal environment.

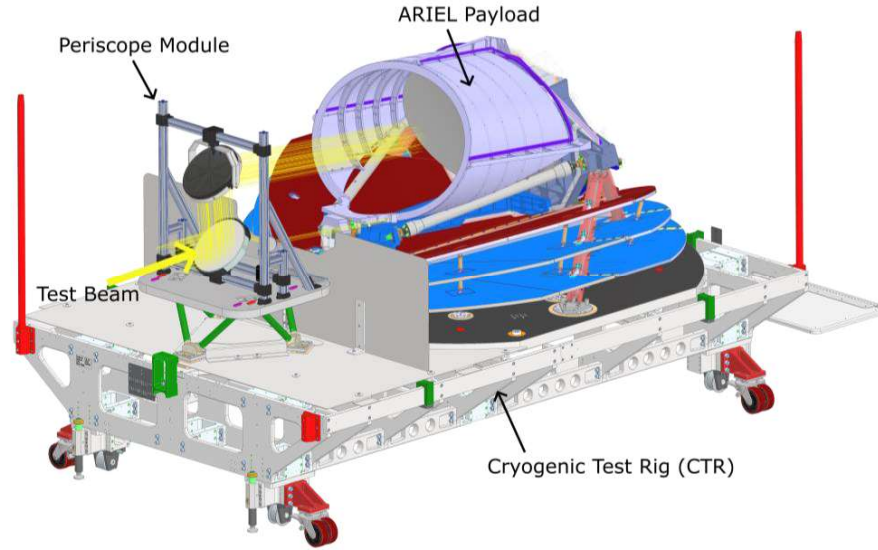


Figure 3: The cryogenic test rig (CTR). Shown without the shroud present.

2 THE DESIGN EVOLUTION OF THE OGSE

The system architecture described in Figure 1 was arrived at after a series of system-level trade-off studies. During Phase A, a double-pass configuration was considered (Figure 4). This followed a JWST-like architecture, as described in [5], [6] and [7]. In this concept, the beam was injected within the payload (between M4 and M5) and the test beam was retroreflected by a ~ 1.2 m diameter flat mirror placed in front of M1. However, the double sampling of the payload WFE caused unacceptable aberrations of the point source at the focal planes (~ 1200 nm RMS). The double sampling of the telescope WFE was particularly problematic under 1g where the payload primary mirror experiences significant distortion due to the required lightweighting. To avoid the double sampling of the payload wavefront error a single pass concept was adopted and is described in detail in [2].

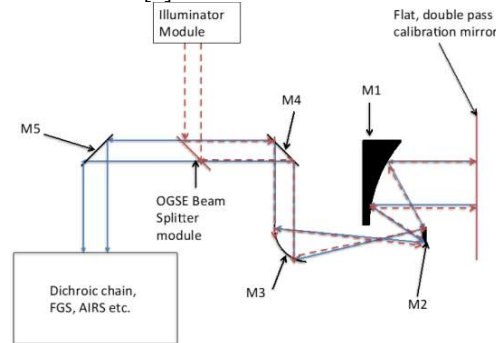


Figure 4: Original Phase A double-pass concept of the OGSE system.

With the single pass architecture, the same illumination module (Figure 4) then injected a beam into a target projector (Figure 5) which expands the illumination module output by 12.5x to give a 275 mm x 183 mm beam at M1. This is, however, $\frac{1}{4}$ the size of the payload pupil. To provide full-aperture illumination of the common optics and instruments mounted behind M1, a beam expander was placed within the payload common optics.

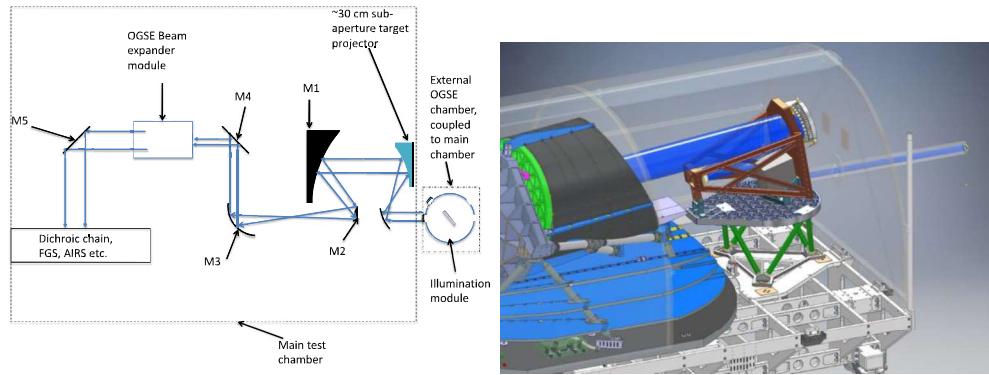


Figure 5: The previous single pass test configuration. Left shows the schematic representation, right shows the CAD model of the target projector concept.

This single-pass approach is somewhat similar to the Euclid approach (described in [8] & [9]). The key difference is that the OGSE for Ariel must be cryogenic in order to prevent the thermal background from saturating the AIRS detectors. This requirement of cryogenic optics is a major complexity driver in particular due to the challenge of maintaining alignment from ambient to cryogenic conditions. A thermoelastic analysis was conducted in order to determine the number of actuated degrees of freedom to align the design described in [2]. It was found that ~11 degrees of freedom would be required to maintain alignment between the different modules as well as to maintain the internal alignment within the target projector. Because of this, the decision was taken to move all the powered optics onto a single optical table in the illumination module. This meant only 4 degrees of freedom of adjustment should be required.

The final change to the system architecture was the removal of the beam expander that was accommodated within the payload (Figure 5). This was largely a trade-off between being able to verify the alignment of the end-to-end system vs fully illuminating the common optics and instruments (providing, for example, a better measurement of the relative defocus between AIRS and FGS). Given Ariel's extremely narrow FOV (~20'') verifying light could reach the focal planes in cryogenic conditions and a flight-like configuration was seen as the more critical test.

3 THE OGSE DESIGN

In section 2, the evolution of the OGSE architecture was described. In the following subsections, we describe in more detail the OGSE design that will be delivered to RAL Space. Returning to the system architecture shown in Figure 1, the OGSE now consists of two modules, the illumination module and the periscope. The cryogenic test rig (CTR) is used to provide a cryogenic radiative environment around the periscope and Ariel payload.

3.1.1 Optical architecture

The illumination module (see Figure 1) generates the test beam used for the calibration and performance verification of the Ariel payload. The illumination module contains two optical benches (see Figure 6): an ambient bench outside the vacuum chamber and a cryogenic bench inside the 1.2m illumination module vacuum chamber. The cryogenic (70 K) optics are necessary to reduce the thermal background in the AIRS CH1 (4-8 micron spectrometer). 70K operation ensures thermal emission contributes less than 1 e/pix/s at the payload detectors.

To minimise the number of vacuum compatible parts and to enable the easy replacement of light sources in the event of a failure, all the light sources (see Figure 6) are accommodated on the ambient bench along with an alignment monitoring system (see section 3.1.2). Three light sources are selectable to be viewed by the payload: a broad band visible source, a broad band IR source and a monochromator (see 3.1.3.1).

The light sources are fed into the chamber via independent windows onto the cryogenic bench where they are injected into the integrating sphere. The integrating sphere also includes reference detectors that monitor changes in source flux. Three types of broadband, single element, detectors are used to cover the full Ariel band width (a MCT, a InSb and a

InGAs detector). Further details on the detectors are provided in [10]. The integrating sphere has two output ports: A 50 μ m pinhole and an open port. The open port provides the uniform illumination required for flat-fielding the payload (see 3.1.3.2). The sphere output is selected by a flip mirror.

The sphere output sits at the object plane of an off-axis parabolic mirror which collimates the output beam. The optical relay after the sphere is shown in Figure 6. An aperture plate (see Figure 6) defines the pupil of the system. The position of this plate ensures that a pupil image lands on M1 (the surface that defines the pupil in flight). After the pupil plate, there are a pair of confocal parabolic mirrors that expand the beam by 7.7 times giving a beam that is $\frac{1}{4}$ aperture with respect to the payload pupil. This design using three powered mirrors ensures:

- (1) The correct output beam size (27.5 x 18.3 cm OGSE pupil)
- (2) The correct plate scale of the pinhole (5381mm effective focal length of the three mirrors).
- (3) An image of the OGSE pupil lands at M1

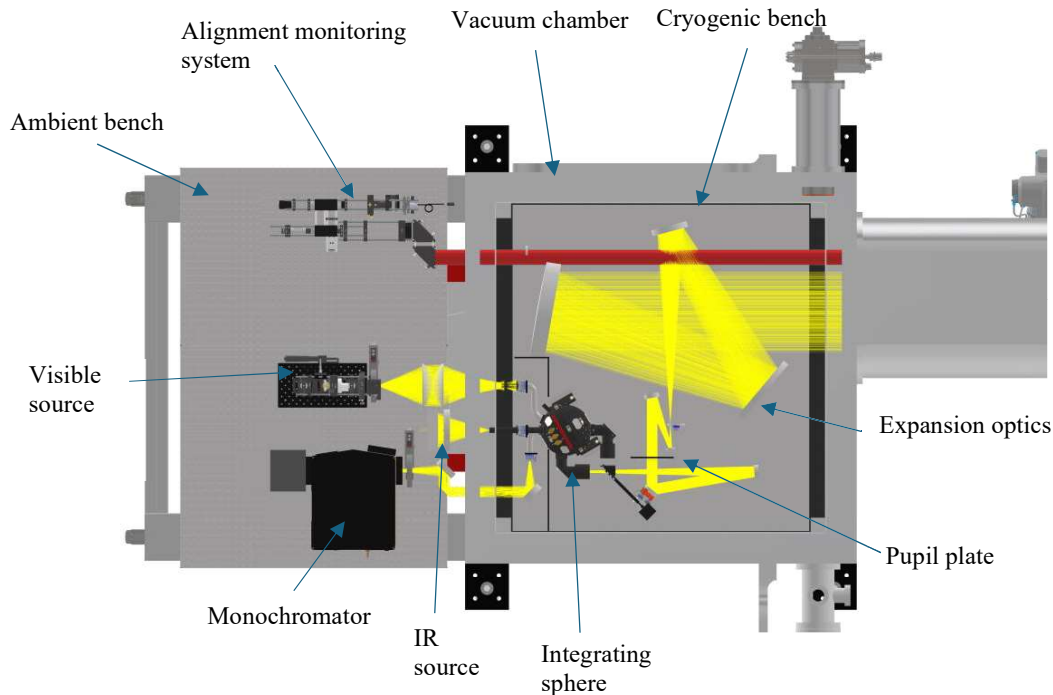


Figure 6: Illumination module architecture

The output of the illumination module is mechanically coupled directly to the RAL 5m chamber via a gate valve. To prevent any reflection ghosts, no window is used at the output of the illumination module.

The illumination module has two output beams: the coherent 532nm autocollimator beam used for alignment and the broadband incoherent test beam. The light from the illumination module is redirected into the line of sight of the Ariel telescope by the adjustable periscope mirrors. Each of the illumination module beams are relayed using its own Z-fold mirror arrangement. The periscope therefore has two smaller (101.6 mm diameter) mirrors to redirect the alignment beam onto the payload alignment cube (UARF1) as well as two larger (340 mm diameter) mirrors to relay the test beam into the payload line of sight.

Each of the periscope mirrors are adjustable in tip-tilt. The two smaller mirrors and the lower large mirror uses manual micrometre screws which are locked and are then removed before T-VAC. The upper mirror remains adjustable at cryogenic temperatures through the use of piezo actuators (see 3.1.2.1).

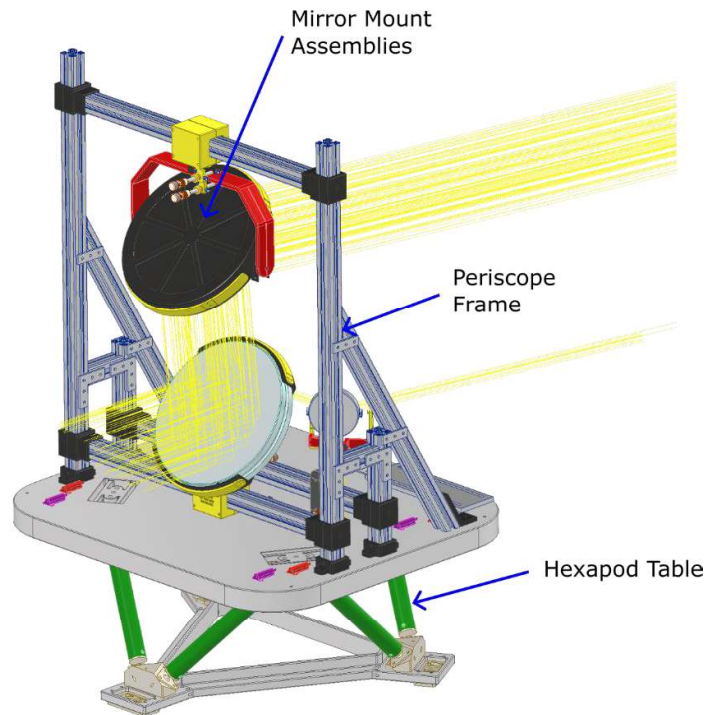


Figure 7: The periscope assembly CAD model

3.1.2 Alignment monitoring and control

Due to Ariel's narrow ($\sim 50''$) FOV, alignment monitoring is particularly challenging, both with regard to establishing the initial alignment and to maintaining this during cooldown. In addition to the narrow field of view, the alignment process is complicated by the payload detectors being inoperable at room temperature, meaning all alignment must be made in a double pass configuration with reflective alignment references and not simply an end-to-end measurement using the payload detectors.

The illumination module includes a custom autocollimator alignment monitoring system (Figure 8) accommodated on the ambient optical bench that can view multiple alignment targets. Using two detector channels, this alignment monitoring system is capable of simultaneously tracking changes in decentre and changes in tip/tilt of the OGSE relative to the payload.

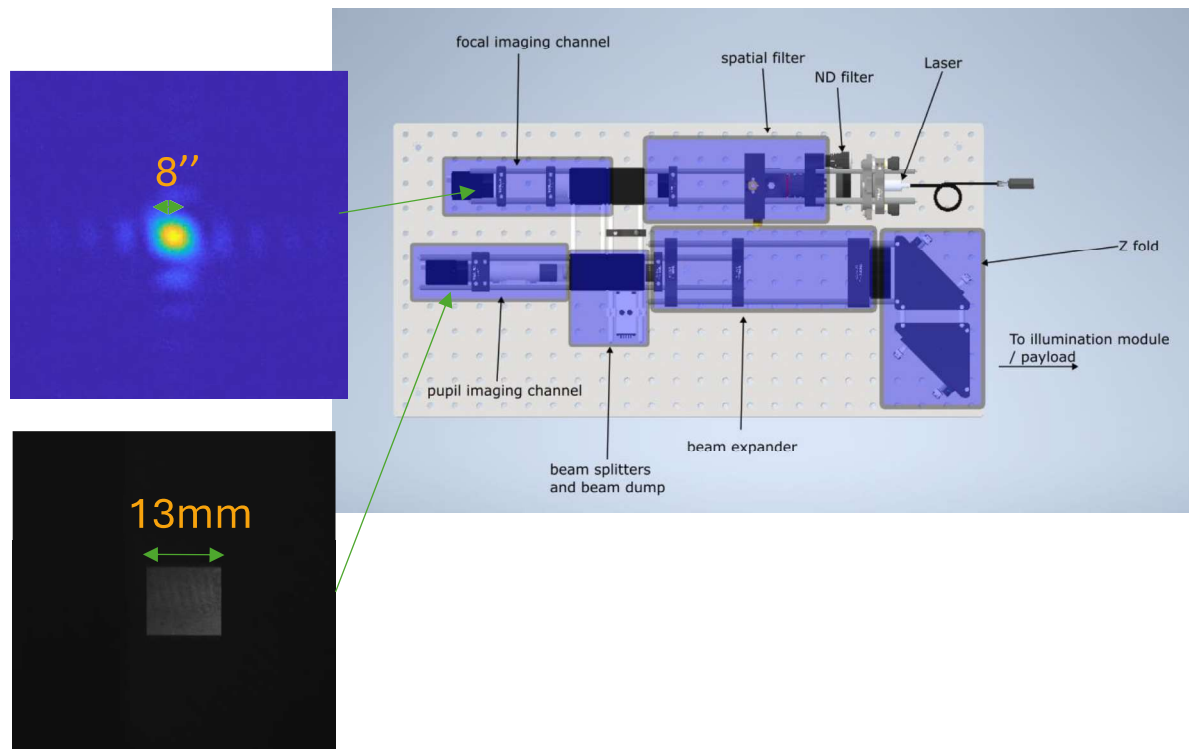


Figure 8: Alignment monitoring system. Figure insets show the measured signal when viewing a payload cube simulator (images are cropped to show the PSF).

Three targets are available to be viewed by the autocollimator:

- (1) The payload alignment cube (shown in Figure 3).
- (2) An off-axis diffuse target located within the payload (at the FGS intermediate focus [4]).
- (3) A reference mirror located on the OGSE cryogenic bench.

The optical path to view each of these targets is shown in Figure 9 (see also Figure 6). Flip mirror 1 is used to redirect the autocollimator to either the payload cube or the test beam path. Flip mirror 2 selects whether the autocollimator or the light from the sphere should be passed through the OGSE expansion optics.

The OGSE reference mirror (3) is used as a proxy for the OGSE optical axis. The goal is to measure the payload line of sight relative to this reference mirror. The payload line of sight can be measured using either of the other two references (the cube or FGS diffuse target). The payload cube serves as a coarse reference for the payload line of sight, with an angular offset which is measured to an accuracy of $15''$ during telescope assembly. The cube is visible over a wide range of field angles ($\pm 750''$), however the optical path to the cube is different from the test beam path, so it is somewhat decoupled from the OGSE optical axis and makes end-to-end alignment verification challenging. For fine alignment, the off-axis target within the payload is used. When this target is seen, it provides a direct measurement that shows the OGSE optical axis is aligned to the payload line of sight. However, this target is only visible over a narrow ($\sim 70''$) range of angles. Moreover, this target requires a view through the telescope optics, so the return signal will be subjected to thermoelastic and gravity-induced aberrations.

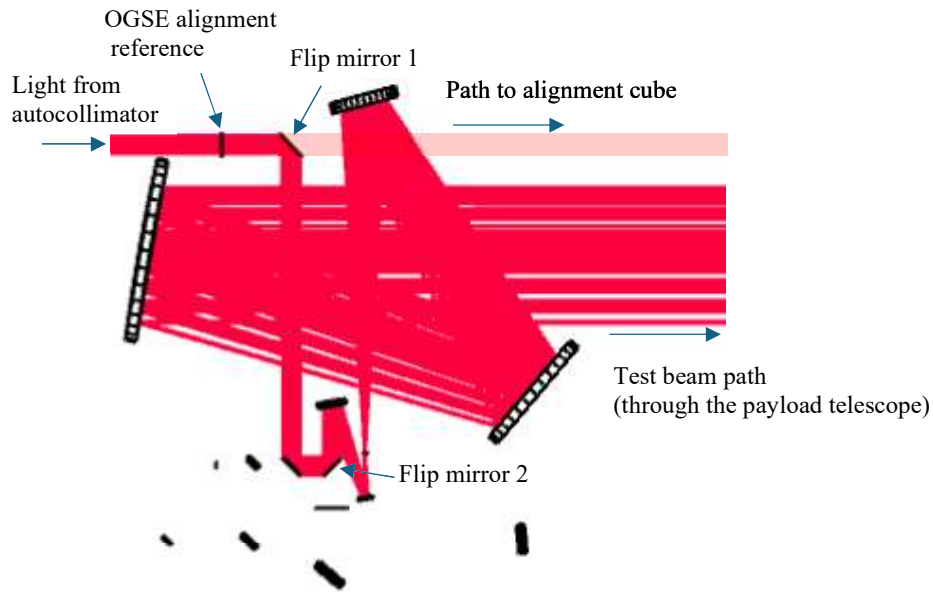


Figure 9: The two autocollimator optical paths. The pink line shows the path to view the payload cube. The red path shows the path through the test beam optics into the payload to be reflected off a target within FGS.

3.1.2.1 Upper mirror assembly

The autocollimator (Figure 8) provides the information necessary to align the OGSE to the payload. However, an adjustment mechanism is required to maintain this alignment during cooldown and the duration of the test campaign. This is achieved by tipping/tilting the upper mirror of the periscope assembly. This is shown in Figure 10. Piezo actuators push against Inconel flexure bearings to provide smooth actuated motion. This is estimated to provide a beam steering range of ± 6.5 degrees with 0.1 arcsecond resolution.

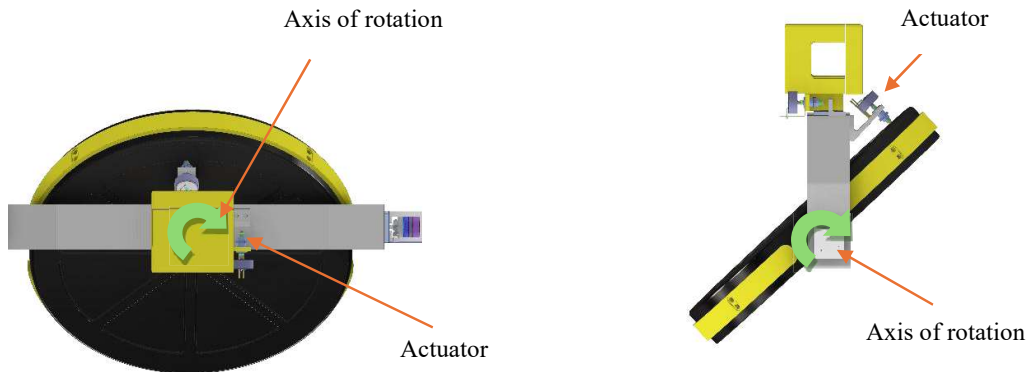


Figure 10: Actuator locations and rotation axes of the upper mirror assembly to enable tip-tilt adjustment.

After initial coarse alignment, it is planned that all motion of the upper mirror will be determined by viewing the FGS reflective target. The FGS target will be illuminated and viewed using the OGSE autocollimator (Figure 9). The upper periscope mirror will be adjusted to keep the FGS target in the centre of the OGSE field of view. However, it is possible

that the OGSE can lose sight of the FGS reflective target during cooldown (e.g. due to a punctuated equilibrium effect). In the event the FGS target is lost, cryo-compatible resistive encoders can be used to raster scan the OGSE beam over a wide range of angles (± 6.5 degrees) until the line of sight is found. These resistive encoders directly measure the bearing angle with 2 arcsecond resolution.

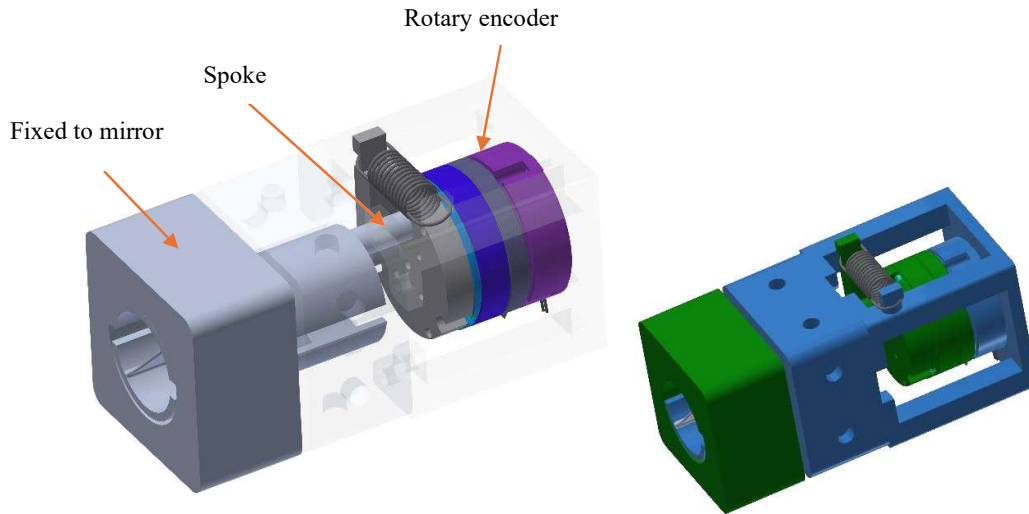


Figure 11: Flexure bearing and rotary encoder. The right figure is used to illustrate the motion of the encoder. Parts that remain fixed are shown in blue. Parts that rotate with the mirror are shown in green.

3.1.3 Illumination modes

Having established the alignment between the OGSE and the payload, the next function of the OGSE is to verify the calibration products derived at lower levels. These calibration products require a range of illumination conditions. The different illumination conditions are enabled by various sources and mechanisms that are summarised in Table 1 and discussed in this section. The modes are not mutually exclusive and are, in many cases, used in combination with other modes listed.

Mode	Design feature	Example applicable test (not exhaustive)
Broad band mode	QTH and Silicon Nitride broad-band sources	Photometric stability
Monochromatic source	Grating monochromator	Wavelength calibration
FGS tracking mode	Short pass filter of the VIS source to illuminate FGS while the monochromator scans	Wavelength calibration
Point source	50 μm pinhole	Co-alignment
Extended source	Open sphere port	Flat field
Rapid shuttering	Voice coil actuated, cryogenic, beam dump	Persistence, dark current
Source monitoring	Reference detectors mounted on the integrating sphere	Photometric stability radiometric calibration
Source modulation	Modulators at the source/ sphere input to allow testing across the full flux range of the payload.	Cross talk/ gain (photon noise limited frames required)
Raster scanning	Actuated periscope mirror	Flat field/ alignment

Table 1: OGSE calibration modes

3.1.3.1 Broadband and monochromatic modes

The OGSE has been designed to provide continuous coverage over a 0.5-7.8 μm wavelength range. The OGSE also provides broadband as well as monochromatic illumination. This is enabled by multiple light sources on the ambient optical bench (Figure 6).

The broadband IR illumination is provided by a Silicon Nitride filament enclosed within an ellipsoidal mirror (Figure 12, Figure 6). The IR source is designed to nominally operate 800K but is capable of operating at up to 1473 K if required. The visible/NIR (<2 μm) broad band illumination is provided by a Quartz-Halogen bulb operating at 3360 K [10]. Monochromatic illumination is achieved using a Czerny-Turner triple grating monochromator. Internal to the monochromator are three further sources: VIS & IR broad-band sources and a discharge lamp.

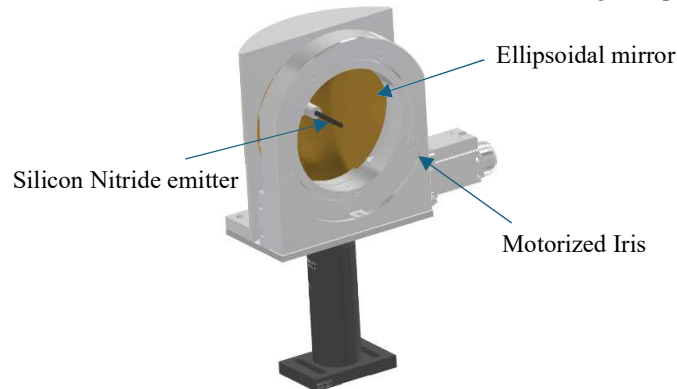


Figure 12: IR source assembly.

Each of the light sources are injected into the integrating sphere via one of three light pipes (Figure 13, Figure 6). The VIS/NIR, IR and monochromator sources can be individually selected or used in combination. To select sources, a cryogenic shutter blade mechanism is used at the entrance of each light pipe (Figure 14). By shuttering in this way, the sources can run continuously throughout the test campaign, negating initial drift when sources are turned on. In addition to the black stop on the shutter blade, the shutter also has other masks that can be placed in the optical path. The open port is used when the point source sphere output is selected. When the extended sphere output is used, the focal plane flux is considerably larger (~100x). To compensate for this, a 1.5mm hole can be selected to attenuate the input flux.

For the VIS source there is an additional mode on the linear stage: a short pass filter. This enables the 'FGS tracking mode'. Measurements such as the wavelength calibration are pointing-sensitive. It is therefore necessary to track the pointing of the test beam whilst the monochromator scans in wavelength. By short-pass filtering the VIS source, the VIS source can be used to only illuminate the FGS photometers for pointing tracking, whilst the monochromator scans over a range of wavelengths.

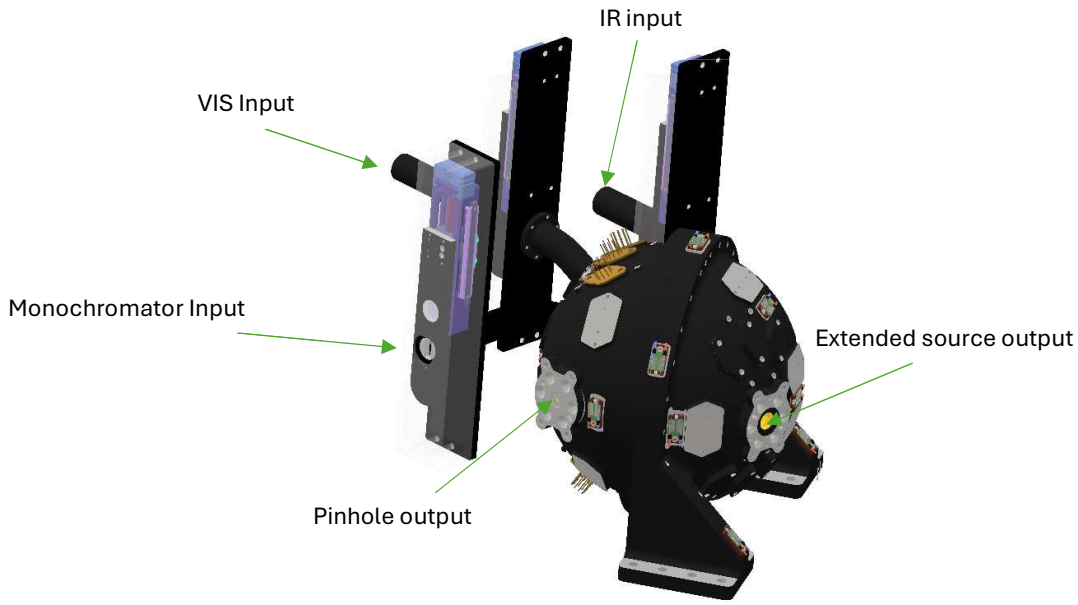


Figure 13: OGSE integrating sphere inputs and outputs

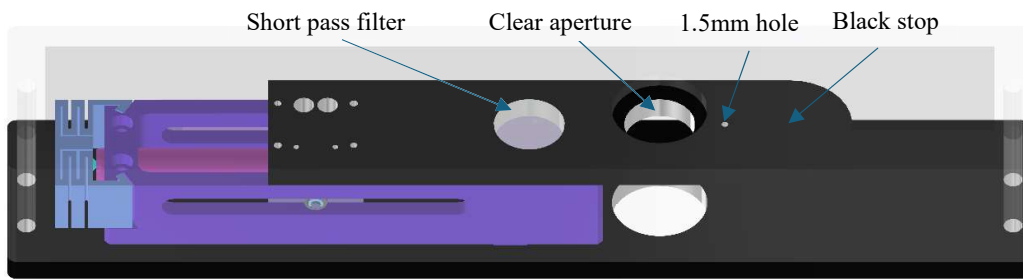


Figure 14: Sphere input shutter assembly

3.1.3.2 Point and extended sphere outputs

Each source described in 3.1.3.1 can be observed as a point source or as an extended source (Figure 13). The output of the integrating sphere is selected using a flip mirror. Each combination of source and sphere output produces different focal plane illumination patterns. Qualitative illustrations of the different observing modes are shown in Figure 15, Figure 16 & Figure 17. These simulations do not include the anticipated ground test aberrations of the payload (primarily gravity-induced).

It should be noted that the extended source will not produce flat illumination when the OGSE illuminates the spectrometers. When a broad-band source with an extended sphere output is used, a spectrum will be seen (Figure 15 – right). When the monochromator is used, an image of the Airs spectrometer slit will be seen (Figure 16 – right). In the absence of any vignetting in the payload, this will produce a top-hat intensity distribution that could be used to produce a local flat field. For the photometers, flat illumination should be possible as shown in Figure 17 (right), again depending on payload vignetting/ field distortion.

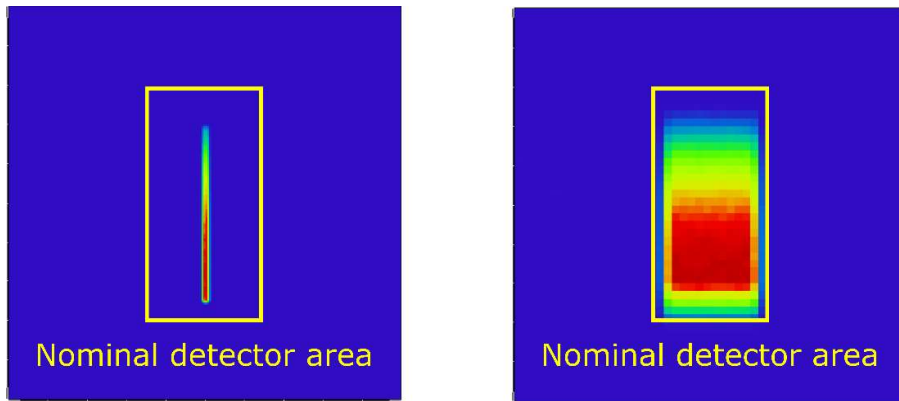


Figure 15: AIRS channel 1 focal plane simulation when illuminated by broad-band sources. Left shows the expected response when the payload is illuminated with a point source. Right shows the focal plane response when the payload is illuminated with an extended source. This figure was generated with a geometric ray trace, i.e. no diffraction

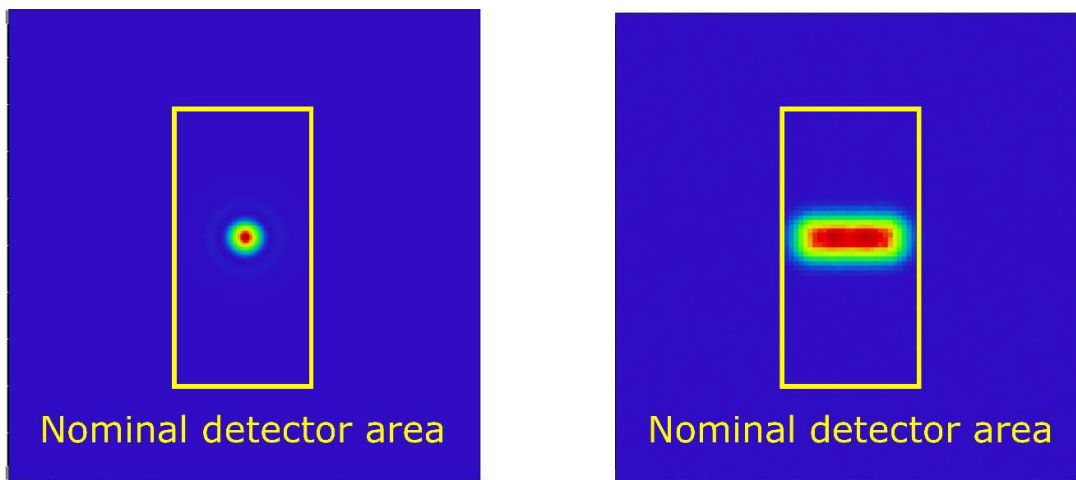


Figure 16: Expected focal plane signal when AIRS is illuminated with the monochromator. Left shows the point source. Right shows the extended source. The location of the spot / top-hat can be scanned by scanning the monochromator wavelength.

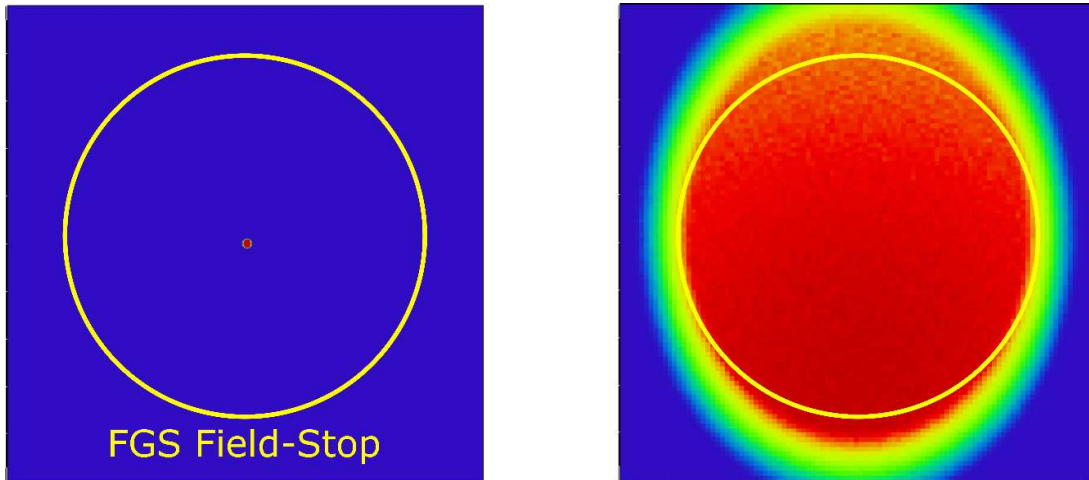


Figure 17: Expected focal plane signal when the FGS photometers are illuminated with point (left) and extended (right) sources. This simulation was evaluated at the FGS intermediate focus.

3.1.3.3 Rapid shuttering

For dark testing of the payload, it is necessary to provide cryogenic (<70K) shuttering of the OGSE. The shutter blades shown in Figure 14 provide the capability to cryogenically shutter each source. In principle, this could be used for dark testing of the payload. However, this would mean the payload would be looking at the reflective sphere surface during dark measurements, likely leading to poor measurements due to stray light. Moreover, the linear blades do not shutter with sufficient speed for persistence measurements. Therefore, when the payload is being dark tested a separate black painted beam dump mechanism will be used. This system is actuated using a voice coil actuator to provide rapid (<<1s) shuttering.

3.1.3.4 Modulation & flux

For all sources, the OGSE has been designed to produce fluxes between the Ariel's brightest and faintest stellar targets (HD219134 and GJ1214, Figure 18). For the broad-band sources, the flux can be tuned between these bright and faint limiting cases using an iris located at the sources. The iris is located before the sphere, so the modulation affects the amplitude without affecting the beam in other ways (e.g. pupil size). For the monochromator, bright target (HD219134) fluxes are not possible. The monochromator is however designed to produce fluxes above the faint target. If required, the monochromator flux can be modulated by tuning the slit width at the cost of spectral linewidth.

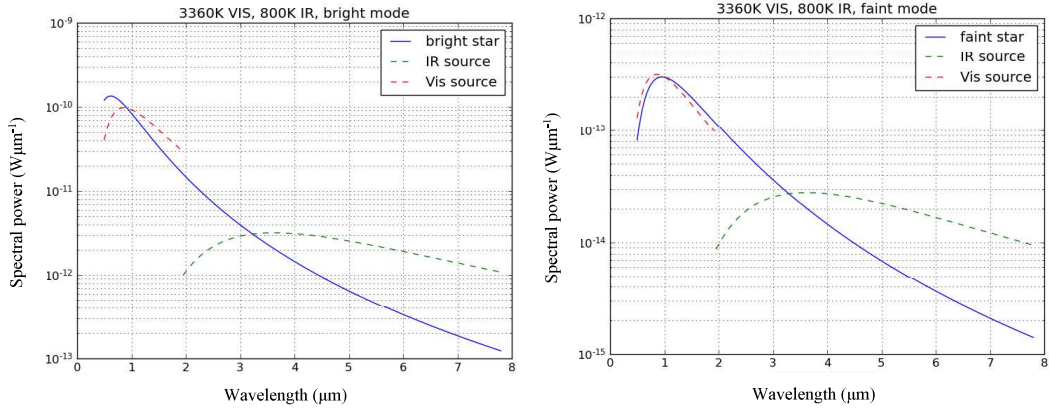


Figure 18: OGSE point source spectral power in the bright (left) and faint (right) observing modes compared to the ARIEL bright and faint stellar targets.

The predicted focal plane saturation times when the payload is illuminated by the various OGSE sources are shown in Figure 19 & Figure 20. These simulations used the ArielRad radiometric model [11].

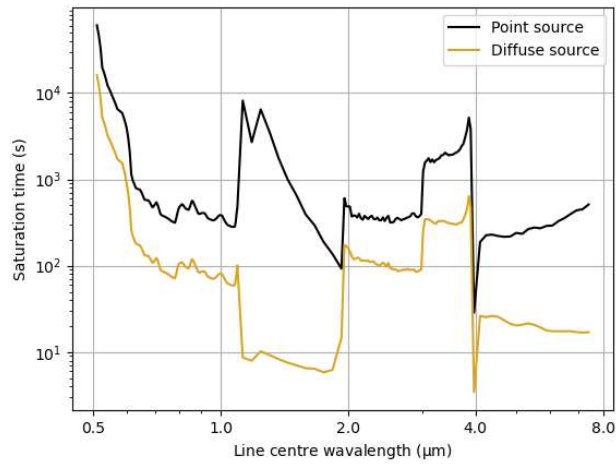


Figure 19: Focal plane saturation times when the payload is illuminated by the OGSE monochromator. Note, these simulations do not include the 1g ground test aberrations.

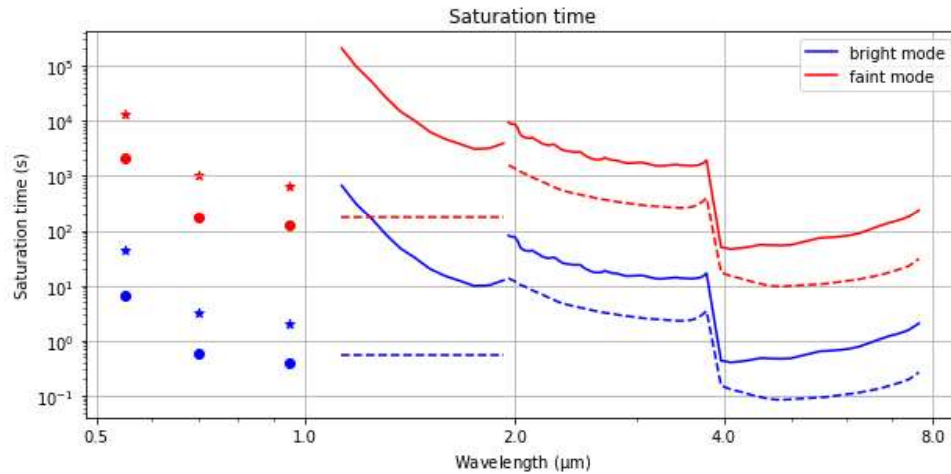


Figure 20: Focal plane signal when the payload is illuminated by the OGSE broadband sources. The diffuse output is shown with the dashed line and stars, the point sphere output is shown with the solid line and dots. The blue shows the limiting bright case, and the red shows the limiting faint case when the source is maximally attenuated. Note, that these simulations do not include the 1g ground test aberrations.

Using the aforementioned mechanisms, a broad range of illumination conditions can be achieved including: point and extended sources; monochromatic and broadband illumination, and bright and faint fluxes, as well as the ability to steer these sources over the payload field of view. This is expected to provide the full range of illumination conditions required to verify the performance of the payload.

4 CONCLUSIONS

In this proceeding the optical equipment for payload level testing of Ariel was presented. Testing a narrow-field ($\sim 50''$), VIS/IR telescope places a number of demanding constraints on the optical test equipment. Two of the most challenging being the alignment maintenance and cryogenic operation. A series of architectures were considered to meet these constraints which led to the current design. The OGSE uses an illumination module to generate a $\frac{1}{4}$ aperture test beam and a periscope to align this beam to the payload. To constrain the motion of the periscope, an alignment monitoring system is used. This uses an autocollimator and a series of reference surfaces to monitor the system's movement. A piezo-driven mirror is then used to compensate for all observed offsets. Finally, the illumination modes of the OGSE system were described. Through a series of actuators, sources, and reference detectors the OGSE is capable of producing the illumination conditions required for performance verification of the payload.

ACKNOWLEDGEMENTS

The Oxford work was funded by a grant from UKSA.

The authors from the University of Lisbon/IA were funded by Fundação para as Ciências e Tecnologias (FCT) through the research grants UIDB/04434/2020 DOI: 10.54499/UIDB/04434/2020 and UIDP/04434/2020 DOI: 10.54499/UIDP/04434/2020 and by the Portuguese Space Agency in the framework of the PRODEX Programme with the European Space Agency (ESA) under contract number PEA 4000129411

REFERENCES

- [1] G. Tinetti *et al.*, "ARIEL Definition Study Report (Red Book)," 2020.
- [2] N. Bowles *et al.*, *Ground calibration of the Ariel space telescope: optical ground support equipment design and description* (SPIE Astronomical Telescopes + Instrumentation). SPIE, 2022.
- [3] J. Martignac *et al.*, *AIRS: ARIEL IR spectrometer status* (SPIE Astronomical Telescopes + Instrumentation). SPIE, 2022.
- [4] R. S. Konrad *et al.*, "ARIEL fine guidance system: design, challenges, and opportunities," in *Proc.SPIE*, 2022, vol. 12180, p. 1218013, doi: 10.1117/12.2629862. [Online]. Available: <https://doi.org/10.1117/12.2629862>
- [5] C. Atkinson *et al.*, *Architecting a revised optical test approach for JWST* (SPIE Astronomical Telescopes + Instrumentation). SPIE, 2008.
- [6] L. Feinberg, J. Hagopian, and C. Diaz, *New approach to cryogenic optical testing the James Webb Space Telescope* (SPIE Astronomical Telescopes + Instrumentation). SPIE, 2006.
- [7] R. Kimble *et al.*, *James Webb Space Telescope (JWST) optical telescope element and integrated science instrument module (OTIS) cryogenic test program and results* (SPIE Astronomical Telescopes + Instrumentation). SPIE, 2018.
- [8] L. Gaspar Venancio *et al.*, *An account of the Euclid payload module test results* (International Conference on Space Optics — ICSO 2022). SPIE, 2023.
- [9] S. Liébecq, "EUCLID Payload Module: Thermal Balance and Thermal Vacuum Test at CSL Premises," in *ECSSMET 2023*, 2023: CNES, Toulouse, France.
- [10] C. Pereira *et al.*, "Stability of the OGSE Vis-NIR illumination sub-system for the future ARIEL space mission," in *SPIE Astronomical Telescopes + Instrumentation*, 2024.
- [11] L. V. Mugnai, E. Pascale, B. Edwards, A. Papageorgiou, and S. Sarkar, "ArielRad: the Ariel radiometric model," *Experimental Astronomy*, vol. 50, no. 2, pp. 303-328, 2020.